

Relationship between iron accumulation and white matter injury in multiple sclerosis: a case–control study

Eytan Raz · Brittany Branson · Jens H. Jensen · Maxim Bester · James S. Babb · Joseph Herbert · Robert I. Grossman · Matilde Inglese

Received: 18 August 2014/Revised: 28 October 2014/Accepted: 31 October 2014/Published online: 22 November 2014
© Springer-Verlag Berlin Heidelberg 2014

Abstract Despite the increasing development and applications of iron imaging, the pathophysiology of iron accumulation in multiple sclerosis (MS), and its role in disease progression and development of clinical disability, is poorly understood. The aims of our study were to determine the presence and extent of iron in T2 visible lesions and gray and white matter using magnetic field correlation (MFC) MRI and correlate with microscopic white matter (WM) injury as measured by diffusion tensor imaging (DTI). This is a case–control study including a series of 31 patients with clinically definite MS. The mean age was 39 years [standard deviation (SD) = 9.55], they

were 11 males and 20 females, with a disease duration average of 3 years (range 0–13) and a median EDSS of 2 (0–4.5). Seventeen healthy volunteers (6 males and 11 females) with a mean age of 36 years (SD = 11.4) were recruited. All subjects underwent MR imaging on a 3T scanner using T2-weighted sequence, 3D T1 MPRAGE, MFC, single-shot DTI and post-contrast T1. T2-lesion volumes, brain volumetry, DTI parameters and iron quantification were calculated and multiple correlations were exploited. Increased MFC was found in the putamen ($p = 0.061$), the thalamus ($p = 0.123$), the centrum semiovale ($p = 0.053$), globus pallidus ($p = 0.008$) and gray matter (GM) ($p = 0.004$) of MS patients compared to controls. The mean lesional MFC was 121 s^{-2} (SD = 67), significantly lower compared to the GM MFC (<0.0001). The GM mean diffusivity (MD) was inversely correlated with the MFC in the centrum semiovale ($p < 0.001$), and in the splenium of the corpus callosum ($p < 0.001$). Patients with MS have increased iron in the globus pallidus, putamen and centrum with a trend toward increased iron in all the brain structures. Quantitative iron evaluation of WM and GM may improve the understanding of MS pathophysiology, and might serve as a surrogate marker of disease progression.

E. Raz · B. Branson · J. H. Jensen · M. Bester · J. S. Babb · R. I. Grossman · M. Inglese
Department of Radiology, New York University Langone Medical Center, New York, NY, USA

E. Raz
Department of Neurology and Psychiatry, Sapienza University, Rome, Italy

J. H. Jensen
Department of Radiology and Radiological Science, Medical University of South Carolina, Charleston, SC, USA

M. Bester
Department of Diagnostic and Interventional Neuroradiology, University Medical Centre Hamburg-Eppendorf (UKE), Hamburg, Germany

J. Herbert
Department of Neurology, New York University Langone Medical Center, New York, NY, USA

M. Inglese (✉)
Department of Neurology, Radiology and Neuroscience, Icahn School of Medicine at Mount Sinai School of Medicine, New York, NY, USA
e-mail: matilde.inglese@mssm.edu

Keywords Multiple sclerosis · Iron · Neuroimaging · MRI · Inflammation

Introduction

Since the observation by Drayer et al. [1] that T2-weighted MRI can indirectly detect increased iron in the basal ganglia of patients with multiple sclerosis (MS), several radiological studies employing different MRI sequences

have confirmed these findings reporting higher concentration of iron in the deep gray matter structures (e.g., caudate nucleus, globus pallidus, putamen, thalamus) of MS patients [2–6].

In addition, these *in vivo* findings are in part supported by the presence of iron at histological examination of brain post-mortem samples from MS patients [7–9].

Despite the increasing development and applications of iron imaging, the pathophysiology of iron accumulation in MS, and its role in disease progression and development of clinical disability, is poorly understood. It has been reported that increased iron is associated with decreased brain volume [10], or in some cases can precede brain atrophy development [11] suggesting its potential contribution to neurodegenerative processes. However, it is not clear whether the increase of iron is a mere consequence of inflammatory demyelinating lesions, whether it has a causative role [12] or whether it has a role at all [13]. We have previously demonstrated the feasibility and sensitivity of magnetic field correlation (MFC), in detecting brain iron increase in the deep GM of MS patients [4]. MFC is a recently developed quantitative MR technique with an iron contrast mechanism, which has a direct relationship with the magnetic field inhomogeneity. Unlike measures of relaxation rates $R2^*$ and $R2$, that are sensitive not only to the presence of iron but also to other relaxation mechanisms such as dipolar interactions, MFC measures the magnetic field shifts such as those generated by iron rich cells with length scales ranging from 1 to 100 μm [14] and depends only on magnetic field inhomogeneities and weakly on water diffusion. Therefore, MFC has a more direct relationship to the magnetic field inhomogeneity, allowing for a more straightforward physical interpretation [15]. Susceptibility weighted imaging (SWI) is another technique employed to evaluate iron deposits; however, SWI uses an arbitrary scaled magnitude image inherently incorporated in the sequence that does not allow any quantitative assessment [15]. Quantitative susceptibility mapping (QSM) has been developed to overcome this limitation by providing voxel intensity linearly proportional to the underlying tissue apparent magnetic susceptibility. Likewise MFC, QSM is limited by a lower accuracy for the evaluation of the white matter, due to the counteracting contribution from diamagnetic myelinated neuronal fibers which confounds the interpretation [15]. Although other tissue features, such as calcifications and myelin content, may conceivably affect the MFC, iron and MFC have been shown to be highly correlated in deep gray matter regions [6, 16–18], which is consistent with the known magnetic properties of ferritin iron (the most common form of iron in brain tissue). In this paper, we accept the hypothesis that MFC is strongly linked to brain

iron, with the caveat that we cannot necessarily exclude other potential contributions.

The aim of our study was threefold: (a) to detect the presence and extent of iron accumulation in T2 visible lesions and gray and white matter in MS patients using MFC MRI; (b) to investigate the relationship between MFC-detected iron accumulation in t GM and the presence of macroscopic inflammation, as measured by the presence of gadolinium-enhancing lesions and microscopic WM injury as measured by diffusion tensor imaging (DTI); (c) to investigate the clinical relevance of brain regional MFC measures.

Materials and methods

Subjects

This is a case–control study of 31 patients with clinically definite MS [19] from consecutive admissions to the MS center of our Hospital. Inclusion criteria were: (a) relapsing–remitting course [20]; (b) no steroid treatment in the prior 30 days; (c) no MRI contraindications. The mean age of the 31 patients was 39 years ($SD = 9.5$), they were 11 males and 20 females, a disease duration average of 3 years (range 0–13) and a median EDSS of 2 (range 0–4.5). Twenty-seven patients were on immunomodulatory or immunosuppressant treatment: 16 patients were under treatment with interferon (IFN) beta, 11 with IFN beta 1b (Betaseron) and 5 with IFN beta 1a (Avonex) 5 patients with glatiramer acetate (Copaxone) and 6 with Natalizumab (Tysabri). Seventeen healthy volunteers (6 males and 11 females) with a mean age of 36 years ($SD = 11.4$), without history of neurological disease and normal brain MRI scans, were recruited as control subjects.

MRI acquisition

All subjects underwent MR imaging on a 3T scanner (Tim Trio; Siemens Medical Solutions, Erlangen, Germany). The body coil was used for signal intensity transmission, and the manufacturer-provided 12-channel head coil designed for parallel imaging was used for signal intensity reception. Section orientation parallel to the subcallosal line was assured by acquiring a multiplanar T1-weighted localizer at the beginning of each study. The MR imaging protocol included the following sequences:

1. Axial T2-weighted FSE sequence ($TR = 5700$ ms, $TE = 113$ ms, matrix = 487×635 , $FOV = 320 \times 320$ mm, section thickness = 3 mm, acceleration factor = 2).

2. Sagittal 3D T1 MPRAGE sequence on 160 contiguous sections (TR = 2300 ms, TE = 3 ms, TI = 900 ms, flip angle = 9°, matrix = 487 × 635, FOV = 240 × 240 mm, section thickness = 1 mm, intersection gap = 0 mm, acceleration factor = 2).
3. Axial MFC by using a segmented (4 shot) EPI asymmetric echo sequence on 48 sections [TR = 5130 ms, TE = 40 ms, matrix = 128 × 128, flip angle = 90°, FOV = 256 × 256 mm, bandwidth = 1346 Hz/pixel, section thickness = 1.7 mm, intersection gap = 0 mm (resulting in isotropic voxels)]. Images were acquired with refocusing pulse time shifts of $t_s = 0, -4, \text{ and } -16$ ms, where the negative sign indicates a reduction of the interval between the initial 90° excitation pulse and 180° refocusing pulse from the usual spin-echo value of TE/2. For each set of imaging parameters, four images were acquired to increase the signal intensity-to-noise ratio [17].
4. Axial DTI using a single-shot EPI with 15 noncollinear directions with $b = 1,000$ s/mm². One image without diffusion weighting ($b = 0$) was acquired for each set of 6 diffusion-encoding directions on 48 3-mm-thick contiguous slices (TR = 8200, TE = 97 ms, matrix = 128 × 128, FOV = 230 × 230 mm, in-plane voxel size 1.8 × 1.8 mm). For each set of imaging parameters, four images were acquired to increase the signal-to-noise ratio.
5. Post-contrast axial T1 SE sequence (TR = 600 ms, TE = 16 ms, matrix = 487 × 635, FOV = 320 × 320 mm, section thickness = 3 mm) was acquired after intravenous injection of gadopentate dimeglumine (Magnevist, Berlex Laboratories, Wayne, NJ) with a standard dose of 0.1 mmol/kg body weight.

MRI analysis

The MR images were transferred off-line and processed by a neuroradiologist and a clinician with more than 5 years experience in MRI post-processing.

Lesion volume

Gadolinium (Gd) enhancing lesions were counted on post-contrast T1-W images by a neuroradiologist blind to subjects' identity. The quantification of lesion volume (LV) was performed both on the T2-W and precontrast T1-W images using a semi-automated method (Jim 4.0; Xinapse System, Leicester, UK) by an MR expert (MI, Board certified in Neurology, with 15 years of experience) and a neuroradiologist (ER, with 7 years of experience). The value of total brain LV was calculated by multiplying lesion area by slice thickness.

Brain volume

Brain volumes were measured on 3D T1-W MPRAGE images by using SIENAX, the cross-sectional version of the SIENA software that is part of FSL [21]. Normalized brain volume (NBV), gray matter volume (GMV) and white matter volume (WMV) were obtained. SIENAX allows global measures with a mean standard error across a group of normal subjects of about 0.5–1 %. To correct for misclassification of T1-W GM volume in presence of high T1-LV [22], each T1-hypointense lesion was filled with the mean intensity value of the NAWM present in the same slice of the lesion to reduce the impact of lesion-associated segmentation bias.

DTI analysis

DTI images were processed using an in-house developed program written in IDL (Exelis Visual Information Solutions, Boulder, Colorado). The diffusion weighted images were first corrected for motion using the linear registration implemented in the Automated Image Registration (AIR) software package (<http://www.bishopw.loni.ucla.edu/AIR5/>). The diffusion tensor (DT) was estimated by linear regression [23] and FA and MD were calculated. To obtain separate WM maps, the affine transformation needed to correct for position between the b0 (without diffusion weighting) images and T2 weighted images was calculated. Normalized mutual information was the similarity chosen for matching. The obtained transformation matrix and a linear interpolation were applied to the quantitative maps. The second step consisted of segmenting the T1 weighted image in GM and WM (Using FAST-FMIRB's Automated Segmentation Tool of FSL). The whole brain T1 images as well as the WM masks were registered to the T2 image as described above.

The T2 lesion mask was subtracted from the WM mask to receive a WM mask of normal-appearing WM (NAWM) exclusively. The quantitative maps were masked with the segmentation results. To exclude pixels with low probability for WM or GM assigned by the segmentation, the maps were thresholded at a value of 0.70 (pixels with computed fraction values >70 % were selected).

Each transformation result was examined individually to exclude errors due to incorrect registration. Histograms with 256 bins were created from these images. To account for variability of brain size, each bin was normalized by the total number of voxels contributing to the histogram. From each histogram the mean value was extracted.

Iron quantification

The post-processing of MFC was performed in Matlab 7.0 (MathWorks, Natick, Massachusetts), using the SPM 5

software (Wellcome Department of Cognitive Neurology, London, England) as described previously in details [16, 17]. For a biologic tissue in an applied magnetic field, the MFC may be defined by the following equation:

$$MFC (|t - t'|) = \gamma^2 \langle \delta B(t) \delta B(t') \rangle$$

with $\delta B(t)$ being the magnitude difference between the total and background fields for a water molecule at a time t and with γ being the proton gyromagnetic ratio [16, 17]. In the equation, the field product within brackets is averaged over all water molecules within a voxel. Because of time translation invariance, the MFC depends only on the time difference. Thus, the MFC provides a quantitative means of characterizing MFIs. After coregistration and smoothing, the four repetitions were averaged for each refocusing shift and the parametric maps of the MFC were generated, determined from a least-squares nonlinear equation by using in-house Matlab scripts.

Using ImageJ (<http://rsbweb.nih.gov/ij/index.html>), standard ellipse-shaped ROIs of the following brain regions were then outlined on T2 images bilaterally and applied on coregistered MFC maps: for the head of the caudate nucleus, thalamus, putamen, globus pallidus, hippocampus, red nucleus, centrum semiovale bilaterally and the splenium of the corpus callosum the ROI were drawn on three contiguous slices; only T2 hyperintense lesions with a diameter of at least 5 mm were included in the analysis to minimize partial volume effect. The number of ROIs on contiguous slices was selected according to each lesion's size. The standard ellipse-shaped ROIs were adjusted in size and orientation depending on the brain area analyzed. The mean MFC value (unit of measure = s^{-2}) and SD of the ROIs were calculated and then averaged over sections and brain side.

Statistical analysis

Mixed model analysis of covariance was used to compare subject groups in terms of regional MFC values adjusted for age and sex. Specifically, the regional MFC measures were modeled as functions of subject group, age, and sex. The correlation structure imparted by the inclusion of multiple MFC values per subject was modeled by assuming data to be correlated only when acquired from the same subject and by allowing the error variance to differ across comparison groups (to eliminate the assumption of variance homogeneity). Analysis of covariance (ANCOVA) was used to compare patients and controls in terms of the MFC levels, NBV, GMV, WMV, MD of WM and GM, FA of WM and GM, EDSS, disease duration, T2-LV, T1-LV and number of Gd-enhancing lesions, adjusted for age and sex. The error variance was allowed to differ across subject

groups to avoid an assumption of variance homogeneity. Only in patients mixed model ANOVA was used to compare MFC of lesions with MFC of GM and WM in patients. Shapiro–Wilk tests applied to the residuals verified the underlying assumption of normality. We also compared male and female patients, in terms of all the measured parameters. For patients and controls separately, we correlated MFC in each region and averaged over GM, WM and lesions with NBV, GMV, WMV, MD of WM and GM, FA of WM and GM, EDSS, disease duration, T2-LV, T1-LV and number of Gd-enhancing lesions. All reported p values are two-sided, and statistical significance is defined as $p < 0.05$. SAS 9.0 (SAS Institute, Cary, North Carolina) was used for all computations.

Results

Lesions and brain volume

All subject included were eligible and underwent all required examinations. No data were missing on any subject. In patients, mean T2-LV was 3.75 ± 8.55 and T1-LV was 0.94 ± 2.31 . Ten out of 31 patients had a total of 20 Gd-enhancing lesions, with a range of 1–4 Gd-enhancing lesions each (median = 1 lesion).

NBV and GMV were significantly lower in patients (1639.8 ± 615.5 ; 855.5 ± 32.50 ml) than controls (1690.8 ± 709.2 ; 885.0 ± 39.7 ml; $p = 0.01$ and $p = 0.008$), whereas WMV was lower in patients (784.2 ± 42.3 ml) than controls (805.8 ± 67.5 ml) but the difference did not reach statistical significance ($p = 0.1$).

Table 1 The mean and standard deviation (SD) of MFC (s^{-2}) in each region in subjects in each group and the p value to compare groups in terms of each measure, adjusted for age and sex

Measure	Brain region	Controls		Patients		p value
		Mean	SD	Mean	SD	
MFC	Head of caudate	310	78	351	72	0.090
	Globus pallidus	835	167	1009	249	0.006
	Putamen	338	92	402	102	0.026
	Thalamus	149	20	166	49	0.091
	Hippocampus	115	41	123	70	0.529
	Red Nucleus	395	127	413	120	0.642
	GM	385	72	453	83	0.003
	Centrum semiovale	122	29	141	36	0.050
	Splenium of CC	123	44	126	52	0.879
	WM	122	23	133	38	0.248

Significant p values are in bold

GM gray matter, WM white matter, SD standard deviation, CC corpus callosum

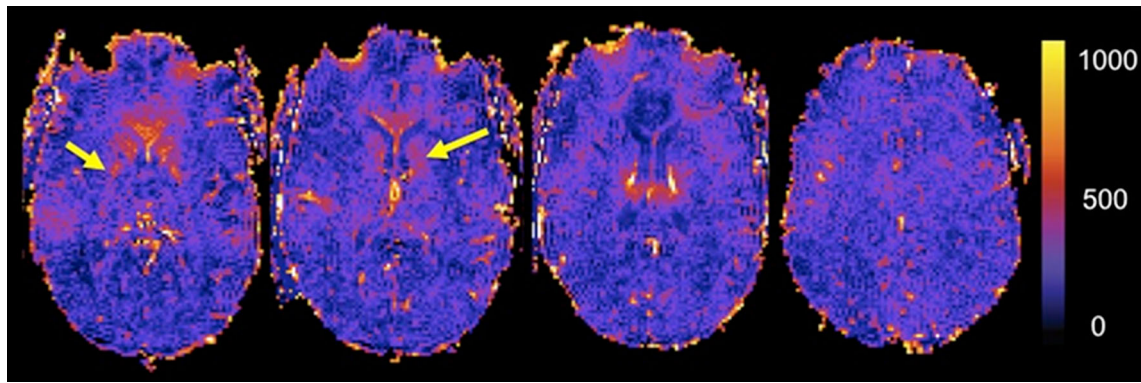


Fig. 1 Selected MFC maps from an MS patient. Note that deep gray matter structures, such as the globus pallidus and the head of the caudate (yellow arrows) show high MFC values (s^2)

DTI

The NAWM MD was significantly higher in patients (0.96 ± 0.05 m/s^2) than controls (0.93 ± 0.02 m/s^2), while there was a trend towards a lower NAWM FA in patients (0.28 ± 0.02) than controls (0.30 ± 0.06 ; $p = 0.051$). GM MD was higher in patients than controls (1.19 ± 0.17 vs. 1.13 ± 0.13 m/s^2) but the difference was not statistically significant ($p = 0.15$).

MFC

Mean and standard deviation of MFC in each brain region examined in patients and controls are presented in Table 1.

In WM lesions, the mean MFC was 121 s^{-2} ($SD = 67$). While these values were significantly lower than those in GM MFC (<0.0001), they were not statistically different from those in NAWM (for MFC $p = 0.608$) (Fig. 1).

Correlation between MFC and lesion and brain volumes

We tested the correlation between MFC in each examined brain region (averaged over GM, WM and lesions) with NBV, GMV, WMV, T2-LV, T1-LV and number of Gd-enhancing lesions. We found a statistically significant association between the MFC value in the thalami and the number of Gd-enhancing lesions ($r = 0.35$; $p = 0.05$) and the MFC value in the head of caudate and NBV ($r = -0.48$; $p = 0.02$) and a trend between the MFC value in the putamen and NBV ($r = -0.45$; $p = 0.06$). Interestingly, when we stratified patients based on the presence of active inflammation as measured by the presence of Gd-enhancing lesions, we found significantly higher MFC values in patients ($n = 10$) with Gd-enhancing lesions compared with patients ($n = 21$) without them (Table 2).

Table 2 The mean (SD) of MFC (in s^{-2}) among patients with and without Gd-enhancing lesions and p values to compare these patient groups using unequal variance t tests

	With Gd-enhancing lesions ($n = 10$)	Without Gd-enhancing lesions ($n = 21$)	p value
MFC			
Whole brain	373 (296)	391 (346)	0.404
GM	430 (305)	465 (358)	0.150
WM	149 (51)	130 (50)	0.005
Lesions	104 (53)	124 (80)	0.020

Bold values are statistically significant

GM gray matter, WM white matter, SD standard deviation

Correlation between MFC and DTI metrics

In patients only, we analyzed the correlation between MFC in each region (averaged over GM, WM and lesions) and MD-WM, FA-WM to evaluate the association of iron with microscopic WM injury. We did not find any significant association between increased MFC in GM regions and diffuse microscopic damages of the NAWM as measured by MD or FA values. We found, however, a significant inverse association between increased GM MD and MFC in the thalamus ($r = -0.4$; $p = 0.03$), in the splenium of the corpus callosum ($r = -0.45$; $p = 0.01$), in the centrum semiovale ($r = -0.38$; $p = 0.05$) and averaged over whole white matter ($r = -0.5$; $p = 0.001$).

Correlation between MFC and demographic and clinical metrics

We did not find any significant association between any MFC-derived metrics in any examined brain regions and age, whereas a significant positive correlation was found between regional GM MFC levels and age in the control group (r ranging from 0.51 and 0.65 and p ranging from

0.01 to 0.005). In patients, there were no significant associations between MFC-derived metrics and disease duration and EDSS score. When we stratified patients based on gender, MFC values (s^{-2}) averaged over gray matter were significantly higher in female (467 ± 356) than male (420 ± 302) patients ($p = 0.04$). However, the significance did not survive when the comparison was corrected for the presence of Gadolinium-enhancing lesions ($p > 0.1$).

Discussion

Using magnetic field correlation, a quantitative MRI technique sensitive to the presence of iron, we found a widespread increase of MFC values in brain gray and white matter regions of MS patients in comparison to healthy controls. However, the increase in MFC reached statistical significance in the globus pallidus, putamen and in the centrum semiovale whereas a trend was observed for all the other examined regions, confirming the results obtained in a prior study [4].

Iron is an essential element for the normal body physiology but, in certain conditions, its accumulation can be toxic and lead to brain damage [24]. In normal brain, iron is stored with ferritin in oligodendrocytes and myelin sheaths; however, when the oligodendrocytes are destroyed, as part of MS pathology, the iron is released in the extracellular space. Once in contact with the acidic environment created by inflammation, the ferritin shell degenerates and free iron is released [8, 25, 26]. Iron-related brain damage in MS may occur by two main mechanisms: free iron leads to an increased production of reactive oxygen species, which ultimately induce cellular death through oxidative damage caused by the formation of free radicals [26]. Free iron increases as well the production of inflammatory mediators, which, in turn, activate macrophages and microglia [26]. Despite evidence of its causative role in promoting brain damage in MS, some authors have suggested that iron accumulation could occur as an epiphenomenon of demyelination, axonal damage and/or neurodegeneration.

Interestingly, we found a higher MFC values in patients with Gd-enhancing lesions. Moreover, the number of Gd-enhancing lesions was directly associated with increased MFC value in the thalamus, suggesting that active inflammation might trigger brain tissue iron accumulation [12]. Increased iron concentration in patients with active disease may be related to different mechanisms, including altered neurotransmitter metabolism of dopamine or glutamate [1]. Indeed, it has been reported that inflammatory cytokines may trigger iron release from oligodendrocytes, similar to the role of TGF- β 1 on astrocytes [9, 27] and that

in inflamed lesions, the ferroxidases such as hephaestin and ceruloplasmin are upregulated [28] leading to increased iron. Furthermore, in active MS lesions iron-containing oligodendrocytes and myelin are destroyed, leading iron in the extracellular space [29, 30] while the ruptured blood–brain barrier allows the passive movement of transferrin with iron in the brain parenchyma. Finally, during inflammatory-induced hypoxia, iron regulatory proteins (IRP1 and IRP2) are upregulated contributing to elevated translation of transferrin receptors and, eventually, to increased cellular iron storage [26].

We found increased MFC values in subcortical gray matter regions such as the globus pallidus and the putamen and a trend toward significantly increased values in the thalamus. This is consistent with the results of our previous [4] and other MRI studies employing different MRI techniques sensitive to the presence of iron such as susceptibility-induced phase imaging [10] or R2* relaxometry [3]. In the normal brain, deep gray matter nuclei are characterized by very high iron levels. Although the reasons for the increased values in MS patients are not clear, several mechanisms have been proposed including the disruption of iron transport in the deep nuclei neurons, enhanced iron uptake following activation of *N*-methyl-D-aspartate receptors, or altered neurotransmitter metabolism [31].

In our study, higher MFC values were found in the regions of NAWM. This is in line with previous MRI studies suggesting that the content of iron in MS patient follows a parabolic curve, it is absent in patients with clinically isolated syndrome (CIS) [3], increases at the beginning of the disease course and tapers down as the disease progresses into the chronic phase [9, 32]. While in patients with early MS, the increased NAWM iron content could be related to decreased myelin and loss of oligodendrocytes, in chronic MS patients one may expect a reduction of non-heme iron within oligodendrocytes and myelin.

We did not find any associations between WM DTI metrics and increased deep GM MFC suggesting that, at least in our group of patients, diffuse WM microscopic injury does not seem to contribute to excessive iron accumulation. Conversely, we found a significant association between increased MFC in the centrum semiovale, in the thalamus and in the splenium of the corpus callosum and increased GM MD, suggesting that excessive WM iron might affect gray matter neurons by retrograde degeneration. These associations have to be interpreted with caution since although MFC in the thalamus and GM MD were higher in patients than controls, the difference was not statistically significant. Indeed, we cannot rule out that both the increased amount of WM MFC and GM MD are epiphenomenon of demyelination, axonal damage and/or neurodegeneration.

It is well known that age-related iron increase occurs from adolescence to adulthood and it has been shown that MFC is sensitive to iron-related changes occurring with aging [33]. Surprisingly, unlike in healthy control subjects, we did not find a significant association between brain MFC levels and age in MS patients. Since we studied patients with early relapsing-remitting MS and relatively short disease duration, the age interval was quite narrow and this might have contributed to the lack of association. In addition, this might be explained by the prevalence of women in our group since it has been shown that the positive correlation between iron levels and age is practically not observed in women [34].

The finding of high iron in the brain is not without clinical practice consequences: it has been debated over the last few years how the therapeutic interventions can be potentially focused in the patients with higher iron using, for example, chelators, inhibitors of iron-related oxidative stress and lipid peroxidation. Some chelators have been demonstrated useful in neurodegenerative disorders [35].

Due to the cross-sectional design of our study, we were not able to investigate the timing and dynamics of iron accumulation. Longitudinal studies are needed to elucidate the pathophysiology of brain iron increase and its role in MS disease progression [14].

For the purposes of this study, we have regarded MFC as an index of brain tissue iron. For the basal ganglia, this correspondence is strongly supported by a high correlation between observed values and post-mortem measurements of iron concentration and is consistent with the known magnetic properties and histological distribution of tissue iron in the brain [17]. Nonetheless, there are other potential contributions to MFC, which may be of particular importance outside the basal ganglia, where iron concentrations tend to be lower. These include myelin, calcifications, and venous blood. For example, it is still unknown how the interaction of the diamagnetic myelin and the paramagnetic iron influences the MFC values. Moreover, MFC, as a measure magnetic field inhomogeneities, may also be affected by the microscopic spatial pattern of iron deposition. Therefore, it should be borne in mind that the MFC, while a well-defined physical property with a close connection to iron is not a direct measure of tissue iron concentration. Therefore, a multimodality approach including relaxation metrics and MFC is advisable when investigating tissue iron deposition.

Conclusion

Using a newly developed quantitative MRI method, we found increased MFC in the putamen, globus pallidus and centrum semiovale of MS patients, likely reflecting

increased brain iron content. Quantitative iron evaluation of WM and GM using MFC as iron biomarker provides insights into the understanding of MS pathophysiology, and might be useful as a surrogate marker of disease progression.

Acknowledgments Funding: This study was supported in part by grants from the National Institute of Health RO1 NS29029 to R.G. and R56 NS051623 to M.I. and funds from the Noto Foundation to M.I.

Conflicts of interest The authors declare that they have no conflict of interest.

Ethical standards This study has been approved by the appropriate ethics committee and has therefore been performed in accordance with the ethical standards laid down in the 1964 Declaration of Helsinki and its later amendments. All persons gave their informed consent prior to their inclusion in the study.

References

1. Drayer B, Burger P, Hurwitz B, Dawson D, Cain J (1987) Reduced signal intensity on MR images of thalamus and putamen in multiple sclerosis: increased iron content? *AJR Am J Roentgenol* 149(2):357–363
2. Bakshi R, Dmochowski J, Shaikh ZA, Jacobs L (2001) Gray matter T2 hypointensity is related to plaques and atrophy in the brains of multiple sclerosis patients. *J Neurol Sci* 185(1):19–26
3. Khalil M, Teunissen C, Langkammer C (2011) Iron and neurodegeneration in multiple sclerosis. *Mult Scler Int* 2011:606807
4. Ge Y, Jensen JH, Lu H, Helpert JA, Miles L, Inglesse M, Babb JS, Herbert J, Grossman RI (2007) Quantitative assessment of iron accumulation in the deep gray matter of multiple sclerosis by magnetic field correlation imaging. *AJNR Am J Neuroradiol* 28(9):1639–1644
5. Hammond KE, Metcalf M, Carvajal L, Okuda DT, Srinivasan R, Vigneron D, Nelson SJ, Pelletier D (2008) Quantitative in vivo magnetic resonance imaging of multiple sclerosis at 7 Tesla with sensitivity to iron. *Ann Neurol* 64(6):707–713
6. Habib CA, Liu M, Bawany N, Garbern J, Krumbein I, Mentzel HJ, Reichenbach J, Magnano C, Zivadinov R, Haacke EM (2012) Assessing abnormal iron content in the deep gray matter of patients with multiple sclerosis versus healthy controls. *AJNR Am J Neuroradiol* 33(2):252–258
7. Craelius W, Migdal MW, Luessenhop CP, Sugar A, Mihalakis I (1982) Iron deposits surrounding multiple sclerosis plaques. *Arch Pathol Lab Med* 106(8):397–399
8. Bagnato F, Hametner S, Welch EB (2013) Visualizing iron in multiple sclerosis. *Magn Reson Imaging* 31(3):376–384
9. Hametner S, Wimmer I, Haider L, Pfeifenbring S, Bruck W, Lassmann H (2013) Iron and neurodegeneration in the multiple sclerosis brain. *Ann Neurol* 74(6):848–861
10. Zivadinov R, Heininen-Brown M, Schirda CV, Poloni GU, Bergsland N, Magnano CR, Durfee J, Kennedy C, Carl E, Hagemeyer J et al (2012) Abnormal subcortical deep-gray matter susceptibility-weighted imaging filtered phase measurements in patients with multiple sclerosis: a case-control study. *Neuroimage* 59(1):331–339
11. Hagemeyer J, Weinstock-Guttman B, Bergsland N, Heininen-Brown M, Carl E, Kennedy C, Magnano C, Hojnacki D, Dwyer MG, Zivadinov R (2012) Iron deposition on SWI-filtered phase in the subcortical deep gray matter of patients with clinically

- isolated syndrome may precede structure-specific atrophy. *AJNR Am J Neuroradiol* 33(8):1596–1601
12. Mehta V, Pei W, Yang G, Li S, Swamy E, Boster A, Schmalbrock P, Pitt D (2013) Iron is a sensitive biomarker for inflammation in multiple sclerosis lesions. *PLoS One* 8(3):e57573
 13. Kilsdonk ID, Lopez-Soriano A, Kuijter JP, de Graaf WL, Castelijns JA, Polman CH, Luijten PR, Geurts JJ, Barkhof F, Wattjes MP (2014) Morphological features of MS lesions on FLAIR* at 7 T and their relation to patient characteristics. *J Neurol* 261(7):1356–1364
 14. Walsh AJ, Blevins G, Lebel RM, Seres P, Emery DJ, Wilman AH (2014) Longitudinal MR imaging of iron in multiple sclerosis: an imaging marker of disease. *Radiology* 270(1):186–196
 15. Ropele S, de Graaf W, Khalil M, Wattjes MP, Langkammer C, Rocca MA, Rovira A, Palace J, Barkhof F, Filippi M et al (2011) MRI assessment of iron deposition in multiple sclerosis. *J Magn Reson Imaging JMRI* 34(1):13–21
 16. Jensen JH, Chandra R, Ramani A, Lu H, Johnson G, Lee SP, Kaczynski K, Helpert JA (2006) Magnetic field correlation imaging. *Magn Reson Med* 55(6):1350–1361
 17. Jensen JH, Szulc K, Hu C, Ramani A, Lu H, Xuan L, Falangola MF, Chandra R, Knopp EA, Schenck J et al (2009) Magnetic field correlation as a measure of iron-generated magnetic field inhomogeneities in the brain. *Magn Reson Med* 61(2):481–485
 18. Raz E, Jensen JH, Ge Y, Babb JS, Miles L, Reaume J, Grossman RI, Inglese M (2011) Brain iron quantification in mild traumatic brain injury: a magnetic field correlation study. *AJNR Am J Neuroradiol* 32(10):1851–1856
 19. Polman CH, Reingold SC, Edan G, Filippi M, Hartung HP, Kappos L, Lublin FD, Metz LM, McFarland HF, O'Connor PW et al (2005) Diagnostic criteria for multiple sclerosis: 2005 revisions to the “McDonald Criteria”. *Ann Neurol* 58(6):840–846
 20. Lublin FD, Reingold SC (1996) Defining the clinical course of multiple sclerosis: results of an international survey. National Multiple Sclerosis Society (USA) Advisory Committee on clinical trials of new agents in multiple sclerosis. *Neurology* 46(4):907–911
 21. Smith SM, Zhang Y, Jenkinson M, Chen J, Matthews PM, Federico A, De Stefano N (2002) Accurate, robust, and automated longitudinal and cross-sectional brain change analysis. *Neuroimage* 17(1):479–489
 22. Battaglini M, Jenkinson M, De Stefano N (2012) Evaluating and reducing the impact of white matter lesions on brain volume measurements. *Hum Brain Mapp* 33(9):2062–2071
 23. Basser PJ, Mattiello J, LeBihan D (1994) Estimation of the effective self-diffusion tensor from the NMR spin echo. *J Magn Reson B* 103(3):247–254
 24. Campbell A, Smith MA, Sayre LM, Bondy SC, Perry G (2001) Mechanisms by which metals promote events connected to neurodegenerative diseases. *Brain Res Bull* 55(2):125–132
 25. Todorich B, Pasquini JM, Garcia CI, Paez PM, Connor JR (2009) Oligodendrocytes and myelination: the role of iron. *Glia* 57(5):467–478
 26. Williams R, Buchheit CL, Berman NE, LeVine SM (2012) Pathogenic implications of iron accumulation in multiple sclerosis. *J Neurochem* 120(1):7–25
 27. Zhang X, Haaf M, Todorich B, Grosstephan E, Schieremberg H, Surguladze N, Connor JR (2005) Cytokine toxicity to oligodendrocyte precursors is mediated by iron. *Glia* 52(3):199–208
 28. Schulz K, Vulpe CD, Harris LZ, David S (2011) Iron efflux from oligodendrocytes is differentially regulated in gray and white matter. *J Neurosci* 31(37):13301–13311
 29. Barnett MH, Prineas JW (2004) Relapsing and remitting multiple sclerosis: pathology of the newly forming lesion. *Ann Neurol* 55(4):458–468
 30. Marik C, Felts PA, Bauer J, Lassmann H, Smith KJ (2007) Lesion genesis in a subset of patients with multiple sclerosis: a role for innate immunity? *Brain* 130(Pt 11):2800–2815
 31. Cheah JH, Kim SF, Hester LD, Clancy KW, Patterson SE 3rd, Papadopoulos V, Snyder SH (2006) NMDA receptor-nitric oxide transmission mediates neuronal iron homeostasis via the GTPase Dexas1. *Neuron* 51(4):431–440
 32. Paling D, Tozer D, Wheeler-Kingshott C, Kapoor R, Miller DH, Golay X (2012) Reduced R2' in multiple sclerosis normal appearing white matter and lesions may reflect decreased myelin and iron content. *J Neurol Neurosurg Psychiatry* 83(8):785–792
 33. Adisetiyo V, Jensen JH, Ramani A, Tabesh A, Di Martino A, Fieremans E, Castellanos FX, Helpert JA (2012) In vivo assessment of age-related brain iron differences by magnetic field correlation imaging. *J Magn Reson Imaging JMRI* 36(2):322–331
 34. Ramos P, Santos A, Pinto NR, Mendes R, Magalhaes T, Almeida A (2014) Iron levels in the human brain: a post-mortem study of anatomical region differences and age-related changes. *J Trace Elem Med Biol* 28(1):13–17
 35. Whitnall M, Richardson DR (2006) Iron: a new target for pharmacological intervention in neurodegenerative diseases. *Semin Pediatr Neurol* 13(3):186–197